

Spectroscopic Evidence for Intramolecular $\text{Mo}^{\text{VI}}(\text{O}_2)\cdots\text{HO}-\text{C}$ Hydrogen Bonding in Solution

Holger Glas, Michael Spiegler, and Werner R. Thiel*

Anorganisch-chemisches Institut, Technische Universität München
Lichtenbergstr. 4, D-85747 Garching
Fax: (internat.) + 49(0)89/289-13473
E-mail: thiel@arthur.anorg.chemie.tu-muenchen.de

Received July 10, 1997

Keywords: Molybdenum / Peroxo complexes / Hydrogen bonds / Catalysis

The ring-opening reaction of epoxycyclohexane with 2-[3(5)-pyrazolyl]pyridine results in the formation of racemic *trans*-2-[3-(2-pyridyl)-1-pyrazolyl]cyclohexanol (**1**). Kinetic resolution with lipase B from *Candida antarctica* gives the (1*S*,2*S*) enantiomer of **1**, the solid-state structure of which was determined by X-ray crystallography, as an enantiomerically pure tridentate ligand. Investigation by NMR spectroscopy of the corresponding oxodiperoxomolybdenum complex **2**, where **1**

acts as a bidentate chelate, proves the formation of a weak intramolecular $\text{Mo}^{\text{VI}}(\text{O}_2)\cdots\text{HO}-\text{C}$ bridge in CHCl_3 solution. This H bonding is broken by solvents such as acetone, THF or DMF, which are capable of forming hydrogen bonds to alcohols. Intermolecular hydrogen bonds between the OH groups and molybdenum peroxo moieties are also found in the solid-state structure of **2**, leading to a helical arrangement of the peroxo complexes.

Peroxo complexes of high-valent transition metals are used as catalysts or stoichiometric reagents for the oxidation of organic and inorganic substrates^[2]. We have investigated the role of seven-coordinate oxodiperoxomolybdenum complexes in the catalytic epoxidation of olefins^[1] and have focused on bidentate *N*-alkylated 2-[3(5)-pyrazolyl]pyridine ligands, first described by H. Brunner et al.^[3]. This ligand system allows the introduction of long alkyl side chains, leading to excellent solubility of the derived molybdenum catalysts in organic solvents, and a variation of the donor strength by the inclusion of electron donating and withdrawing groups attached to the heteroaromatic rings. The latter feature enables a correlation of electronic ligand properties with epoxidation activities of the catalysts^[1]. From spectroscopic and kinetic investigations on peroxo complexes bearing olefinic side chains, we postulated a new reaction mechanism for the catalytic olefin epoxidation with seven-coordinate peroxomolybdenum complexes. In this mechanism the oxidizing agent (e.g. *tert*-butyl hydroperoxide) is activated by the Lewis acidic transition-metal center, resulting in an oxygen transfer from the hydroperoxide, and not from the η^2 -coordinated peroxo ligands, to the olefin^[4].

One crucial point of this mechanism is a proton transfer from the hydroperoxide to one of the peroxo ligands. NMR investigations (¹H, ¹³C, ¹⁷O NMR) on the reactivity of peroxomolybdenum complexes in the presence of strong Lewis and Brønsted acids, showed that the peroxo ligands are preferentially protonated while the oxo ligand is a poor pro-

ton acceptor^[5]. These spectroscopic findings are in agreement with the results of Extended Hückel calculations on the model complex $(\text{NH}_3)_2\text{MoO}(\text{O}_2)_2$, which proved that the three highest occupied molecular orbitals of such compounds possess mainly π^* character at the peroxo ligands and only low σ^* and π^* character at the oxo ligand. From a mechanistic point of view, this proton transfer should start with the formation of a hydrogen bond between the hydroperoxide and an η^2 -peroxo ligand. Since we were never able to prove such interactions between the weak Brønsted base $\eta^2\text{-O}_2$ and weak Brønsted acids like hydroperoxides or alcohols by means of spectroscopy, the energies of these bonds should be low. To overcome this problem, we synthesized new *N,N*-donor ligands of the pyrazolylpyridine type bearing OH functions in the side chain, which should lead to the formation of an intramolecular hydrogen bond. In the present paper, we describe the synthesis of such ligands and the corresponding peroxomolybdenum complexes, along with the NMR- and IR-spectroscopic evidence for a weak intramolecular $\text{Mo}^{\text{VI}}(\text{O}_2)\cdots\text{H}-\text{OR}$ interaction in solution.

Results and Discussion

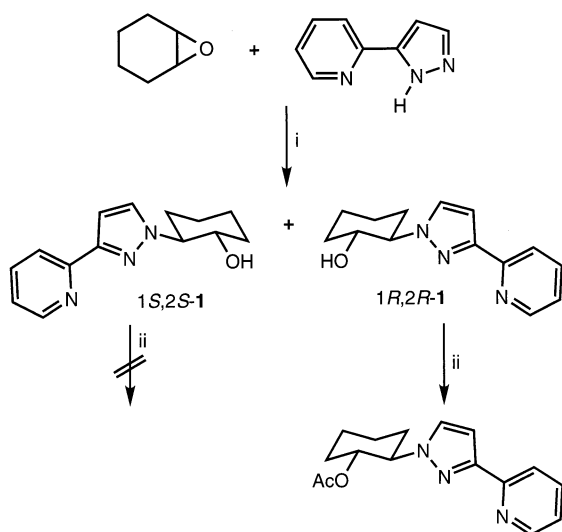
The *N*-alkylation of 2-[3(5)-pyrazolyl]pyridines is usually carried out by a deprotonation (NaH) alkylation (RX, X = Br, I) sequence with THF as the solvent^[6]. According to this procedure, primary linear alkyl substituents can be introduced with high regioselectivities and high yields. From geometric considerations, intramolecular hydrogen bonding would require a 2-hydroxyethyl or a 3-hydroxypropyl group, which can easily be attached to the pyrazole moiety of the

[◇] Part 6: Ref.^[1].

chelate ligand by nucleophilic ring opening of oxiranes or oxetanes. For synthetic reasons we focused on the ring opening of epoxycyclohexane with pyrazolylpyridine, generating a 1,2-disubstituted cyclohexane ring, which would also be expected to increase solubility of the desired peroxo complexes.

Heating a 1:1.5 mixture of 2-[3(5)-pyrazolyl]pyridine and epoxycyclohexane for 4 h at 170°C in a pressure tube^[7] gives *rac-trans*-2-[3-(2-pyridyl)-1-pyrazolyl]cyclohexanol (**1**) in more than 90% yield (Scheme 1).

Scheme 1. i. 160°C, 4 h, pressure tube; ii. isopropenyl acetate, molecular sieve 4 Å, lipase B from *candida antarctica*, 37°C, 4 h

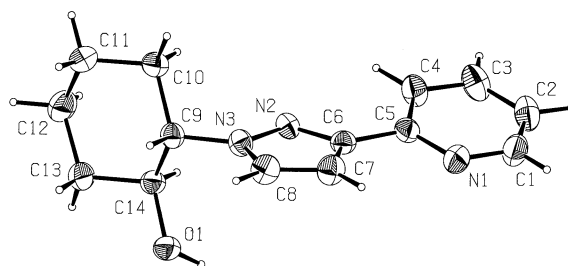


As the resonances of the two protons connected to the substituted cyclohexane carbon atoms are observed at almost identical δ values, the conformation of the aliphatic ring system cannot be determined by means of NMR spectroscopy. However, we expect the cyclohexane ring to occupy the thermodynamically favored chair conformation with both substituents oriented in an equatorial position, as found in similar compounds^[8].

Since we are interested in such compounds as enantiomerically pure ligands for enantioselective catalysis and as starting material for the synthesis of chiral ligands^[9], we investigated the kinetic resolution of **1**^[10]. Acylation of **1** with isopropenyl acetate in the presence of lipase B from *Candida antarctica*^[11] selectively leads to the formation of the acetate with the (1*R*,2*R*) configuration (Scheme 1), which can be separated from (1*S*,2*S*)-**1** by preparative MPLC. The absolute configuration of the non-acylated derivative was determined by X-ray-crystallographic methods (see below). For the corresponding 2-pyrazolylcyclohexanol, an identical stereoselectivity of the enzymatic esterification was found^[10]. Figure 1 shows the molecular structure of (1*S*,2*S*)-**1** in the solid state, along with characteristic bond lengths and angles. Further crystallographic and experimental details are given in Table 1 in the Experimental Section.

(1*S*,2*S*)-**1** crystallizes from diethyl ether at 4°C in the monoclinic space group $P2_1$ with one additional molecule

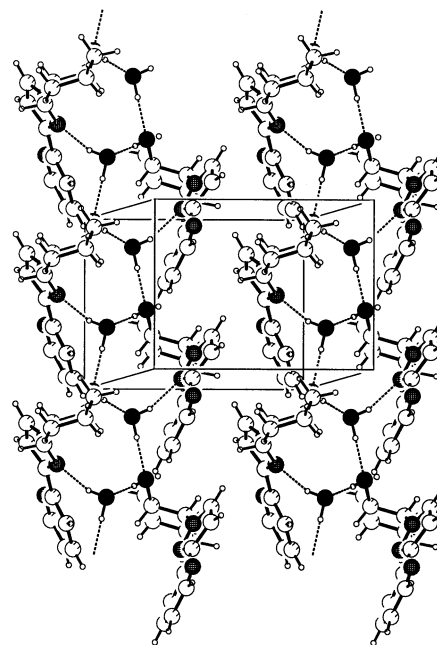
Figure 1. PLATON plot^[12] of (1*S*,2*S*)-**1** (the additional water molecule has been omitted); thermal ellipsoids are at the 50%-level^[a]



^[a] Bond lengths [Å] angles [°] and dihedral angles [°]: N(1)–C(1) 1.332(3), N(1)–C(5) 1.339(2), N(2)–N(3) 1.357(2), N(2)–C(6) 1.342(2), N(3)–C(8) 1.350(2), N(3)–C(9) 1.464(2), C(1)–C(2) 1.386(3), C(2)–C(3) 1.376(3), C(3)–C(4) 1.384(3), C(4)–C(5) 1.386(2), C(5)–C(6) 1.478(2), C(6)–C(7) 1.405(3), C(7)–C(8) 1.359(3), C(9)–C(10) 1.534(3), C(9)–C(14) 1.526(3), C(10)–C(11) 1.523(3), C(11)–C(12) 1.524(3), C(12)–C(13) 1.528(3), C(13)–C(14) 1.516(3), O(1)–C(14) 1.431(2), O(1)–H(1A) 0.91(3), O(1)–H(2B) 1.87(3), O(2)–H(1A) 1.82(3), O(2)–H(2A) 0.87(3), N(2)–H(2A) 2.10(3), O(2)–H(2B) 0.94(3); C(14)–O(1)–H(1A) 110.7(19), H(2A)–O(2)–H(2B) 96.48(11), O(1)–H(1A)–O(2) 172(3), O(2)–H(2A)–N(2) 160(3), O(2)–H(2B)–O(1) 180(3); N(1)–C(5)–C(6)–N(2) –168.96(17).

of water per formula unit. In the solid state structure of enantiomerically pure 2-pyrazolylcyclohexanol^[10], the molecules are linked by hydrogen bonds between the hydroxy groups and the pyrazole moieties, resulting in a helical arrangement. In the case of (1*S*,2*S*)-**1**, this kind of molecular organization is hampered by the bulky pyridyl ring. Therefore, an additional molecule of water is incorporated, forming a new system of hydrogen bonds, which includes the OH group of the cyclohexanol fragment as proton donor and acceptor and the pyrazolyl moiety (N2) of (1*S*,2*S*)-**1** as an acceptor site (Figure 2).

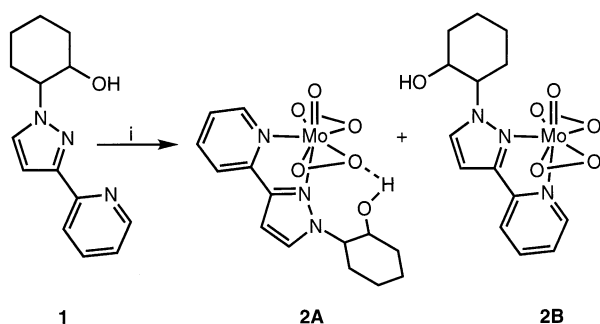
Figure 2. PLUTON plot^[12] showing the hydrogen-bonding system, which builds the solid-state structure of (1*S*,2*S*)-**1**



The structure is best described by an arrangement of water molecules around the crystallographic 2_1 axis, linking the (pyridyl)pyrazolylcyclohexanol molecules to form infinite columns. For reasons of optimization of electronic interaction between the pyridine and the pyrazole ring and steric repulsion between the protons at C4/C7 and the lone pairs at N1/N2, the heteroaromatic rings are twisted by about 10° from coplanarity. All intra- and intermolecular bond lengths and angles were observed as expected. The absolute structure was determined by refinement of the Flack parameter $\chi = -0.061(0.2)^{[13]}$. The refinement of the enantiomorphic structure model with (1*R*,2*R*)-**1** resulted in higher *R* values ($R_1 = 0.035$, $\omega R_2 = 0.098$) and a Flack parameter $\chi = 1.003(0.2)$.

The treatment of *rac*-**1** and (1*S*,2*S*)-**1** with an excess of molybdic acid (hydrated MoO_3), dissolved in H_2O_2 , results in the formation of the seven-coordinate peroxo complexes *rac*-**2** and (1*S*,2*S*)-**2** (Scheme 2).

Scheme 2. i. $\text{MoO}_3 \cdot (\text{H}_2\text{O})_x$, H_2O_2 , room temp., 4 h



Owing to the two different donor centers of the pyrazolylpyridine ligands, the seven-coordinate peroxomolybdenum complexes can exist in two isomeric forms (**A** and **B**). By means of NMR spectroscopy it was found that these isomers are in equilibrium in solution^[14]. In a detailed study, we recently showed that the isomer ratios correlate with the individual donor properties of the heterocyclic ring systems^[1].

Solutions of *rac*-**2** and (1*S*,2*S*)-**2** show the same behavior, which does not depend on the electronic properties of the ligand, but on the nature of the solvent. In chloroform, only isomer **A** can be detected, whereas in donor solvents capable of forming hydrogen bonds with alcohols, like acetone, the isomers **A** and **B** can be observed as expected in a 2:1 ratio. Thus, the electronic characteristics of the chelate ligand cannot be the reason for the special structural feature of **2** in solution in CHCl_3 . We therefore believe an intramolecular hydrogen bond to be responsible for this behavior.

From investigations on the isomer ratios (**A**:**B**) of peroxomolybdenum complexes bearing pyrazolylpyridine ligands with electron-withdrawing and -donating substituents^[1], we can estimate the enthalpy of the intramolecular hydrogen-bond formation to be at least -8 kJ/mol, which corresponds to data from the literature on the thermodynamics of hydrogen bonds between alcohols and ketones ($\Delta G \approx -12$ to -24 kJ/mol)^[15].

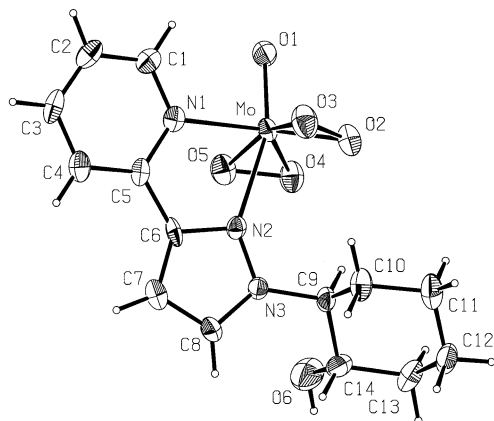
Infrared-spectroscopic investigations at low concentrations (3 mM) in solution support the formation of an intramolecular hydrogen bond: cyclohexanol gives a sharp O–H absorption at 3611 cm^{-1} in chloroform, but a shift of about 100 cm^{-1} towards lower wave numbers is observed in acetone solution, leading to a broad band at 3514 cm^{-1} , typical for associated O–H groups. In contrast to these findings, the IR spectra of **2** in solution, which again show broad O–H absorptions, differ only slightly on a change in the nature of the solvent [chloroform: $\nu(\text{O–H}) = 3491\text{ cm}^{-1}$; acetone: $\nu(\text{O–H}) = 3509\text{ cm}^{-1}$]. This fact provides strong evidence for the formation of hydrogen bonds in both cases: intramolecular in chloroform and intermolecular $[\text{OH} \cdots \text{O}=\text{C}(\text{CH}_3)_2]$ in acetone solution. The intramolecular hydrogen bond could alternatively be formed between the OH group of the chelate-ligand side chain and the oxo or one of the $\eta^2\text{-O}_2$ ligands coordinated to molybdenum. In acetone solution, **2** shows two $\text{Mo}=\text{O}$ stretching vibrations: one at 956 cm^{-1} and an intense shoulder at 950 cm^{-1} , which can be assigned to the two isomers **A** and **B**. The asymmetric and symmetric O–O stretching vibrations are observed at 877 and 868 cm^{-1} for both isomers. In CHCl_3 , the $\text{M}=\text{O}$ absorption at 950 cm^{-1} almost vanishes, while the other $\text{M}=\text{O}$ vibration is shifted to 962 cm^{-1} , indicating an almost selective formation of one isomer. The two O–O absorptions are shifted to lower wave numbers (875 and 865 cm^{-1}), indicating slightly weakened O–O bonds, which would agree with hydrogen bonding to a $\eta^2\text{-O}_2$ ligand. A reduction in the donor capability of the peroxo ligands can be compensated by increased π -backbonding from the oxo ligand to the molybdenum center, as confirmed by the shift of the $\text{Mo}=\text{O}$ stretching frequency to higher wave numbers. However, hydrogen bonding to the oxo ligand would weaken the $\text{Mo}=\text{O}$ bond and therefore shift the $\text{Mo}=\text{O}$ absorption to lower wave numbers. The $\text{Mo}=\text{O}$ and O–O absorptions of peroxomolybdenum complexes bearing pyrazolylpyridine ligands with unfunctionalized alkyl side chains, like [2-(3-butylpyrazol-1-yl)pyridine]oxodiperoxomolybdenum(VI)^[6], which cannot participate in any intramolecular hydrogen bonding, show only weak solvent dependences [acetone: $962, 957\text{ cm}^{-1}$ ($2 \times \nu_{\text{Mo}=\text{O}}$), $877, 868\text{ cm}^{-1}$ ($2 \times \nu_{\text{O}=\text{O}}$); CHCl_3 : $963, 956\text{ cm}^{-1}$ ($2 \times \nu_{\text{Mo}=\text{O}}$), $878, 866\text{ cm}^{-1}$ ($2 \times \nu_{\text{O}=\text{O}}$)].

From these results, it is clear that the intramolecular hydrogen bond should be formed between the OH group (H^+ donor) and one $\eta^2\text{-O}_2$ ligand (H^+ acceptor) in CHCl_3 solution, and this is in agreement with spectroscopic investigations of peroxomolybdenum complexes in the presence of strong Lewis and Brønsted acids^[5]. This interaction would favor an orientation of the pyrazole moiety *trans* to the oxo ligand (isomer **A**, Scheme 2). However, this geometry is not in accordance with the assignments of the spectra of these complexes, which we published in previous papers^{[1][4][5][6]}, a contradiction which had to be clarified.

Crystallization of *rac*-**2** from chloroform gives yellow needles and a small amount of yellow plates ($< 5\%$). Investigations of the needle-like material by X-ray crystallography indicated the solid-state structure of *rac*-**2**, which

crystallizes in the orthorhombic and acentric space group $Pca2_1$. Figure 3 shows the molecular structure of *rac-2* along with bond lengths and angles. Further crystallographic and experimental details are given in Table 1 in the Experimental Section.

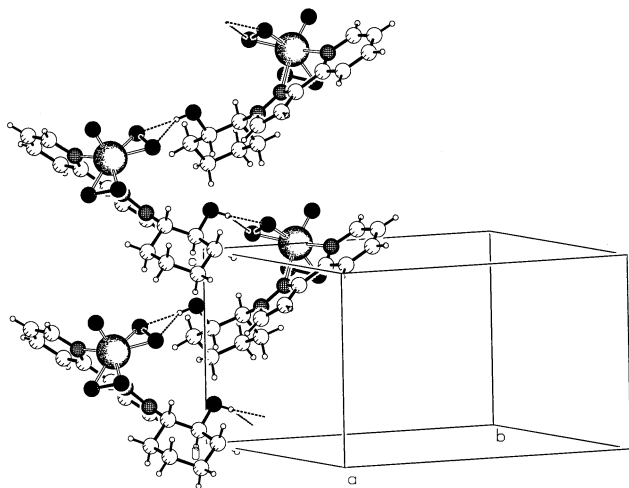
Figure 3. PLATON plot^[12] of the asymmetric unit of *rac-2*; thermal ellipsoids are at the 50-% level^[a]



^[a] Bond lengths [Å] angles [°] and dihedral angles [°]: Mo–O(1) 1.675(5), Mo–O(2) 1.898(3), Mo–O(3) 1.951(5), Mo–O(4) 1.899(4), Mo–O(5) 1.955(4), Mo–N(1) 2.224(3), Mo–N(2) 2.347(4), O(2)–O(3) 1.457(5), O(4)–O(5) 1.467(5), O(6)–H(6A) 0.820, O(6)–C(14) 1.419(7), O(4)–H(6A) 2.532, O(5)–H(6A) 2.010; O(1)–Mo–O(2) 105.1(2), O(1)–Mo–O(3) 102.0(2), O(1)–Mo–O(4) 104.9(2), O(1)–Mo–O(5) 98.9(2), O(1)–Mo–N(1) 90.2(2), O(1)–Mo–N(2) 160.3(2), O(2)–Mo–O(3) 44.5(2), O(4)–Mo–O(5) 44.7(2), N(1)–Mo–N(2) 70.3(2), O(6)–H(6A)–O(4) 139.0, O(6)–H(6A)–O(5) 171.4; C(6)–N(2)–N(3)–C(8) 0.5(5).

Only isomer **A** is found in the solid-state structure, with pyrazole *trans* to the oxo ligand, like it is observed in CHCl_3 solution. However, in the solid state the hydrogen bond is not *intra*- but *intermolecular* between the OH group and an $\eta^2\text{-O}_2$ ligand, linking two peroxomolybdenum complexes and finally leading to the formation of a helical arrangement (Figure 4). The crystals include helices of opposite chirality.

Figure 4. PLUTON plot^[12] of the helical arrangement formed by hydrogen bonding in the solid-state structure of *rac-2*



Clearly, intermolecular hydrogen bonding is energetically favored in the solid state with respect to the intramolecular mode observed in solution. Besides the $\text{OH}\cdots\text{O}_2$ bond, which has previously been observed in the solid-state structure of only one other high-valent transition-metal peroxo compound^[16], *rac-2* shows the typical structure of a molybdenum oxodiperoxo fragment coordinated to a bidentate N,N' -ligand^{[4][6][17]}. Owing to the *trans* influence of the oxo ligand, the distance Mo–N2 is about 12 pm larger than Mo–N1. The peroxo ligands are bent with respect to the oxo ligand, leading to a distorted pentagonal-bipyramidal coordination geometry.

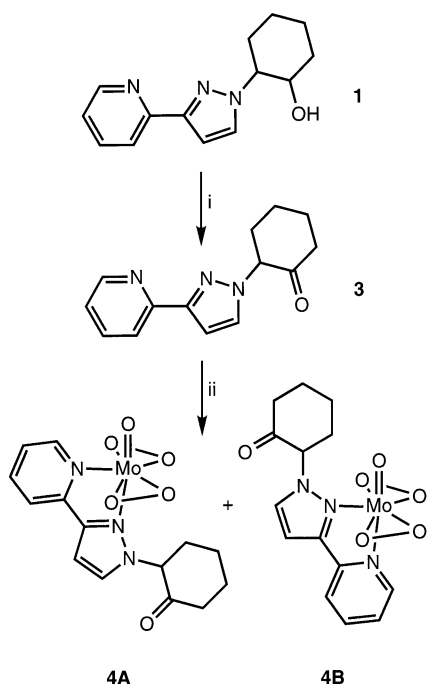
An analogous structure was found for the second type of crystalline material (yellow plates) in which pyrazole is *trans* to the oxo ligand. Owing to the poor crystal quality and a severe problem of disorder concerning the orientation of the OH group at the cyclohexane ring relative to the mirror plane of the $\text{MoO}(\text{O}_2)_2$ fragment, it was not possible to finish the structure refinement with acceptable R values ($R_1 = 0.0993$, $\omega R_2 = 0.2780$)^[18].

For the final assignment of the spectroscopic data of **2**, we carried out powder-diffraction and solid-state NMR experiments. Powder diffraction of the solid material, either crystalline or microcrystalline, can be correlated with the crystal data of the single-crystal diffraction experiment (space group $Pca2_1$) and, in addition, ^{13}C CPMAS experiments gave only one set of resonances. Therefore, the NMR spectra of the peroxo complexes in solution can now be assigned correctly (see Experimental Section). As shown in Scheme 2 the pyrazole fragment in isomer **A** is oriented *trans* to the oxo ligand.

The peroxo complexes **2** catalyze the epoxidation of olefins in the presence of *tert*-butyl hydroperoxide. Detailed investigations on the epoxidation of prochiral olefins with (1*S*,2*S*)-**2** unequivocally showed that racemic epoxides are formed under standard conditions (50°C, CHCl_3). The hydroxy group of the ligand remains unaffected during these reactions, which is in agreement with findings in the literature that neutral peroxomolybdenum complexes do not catalyze the oxidation of alcohols. In contrast, alcohols are preferentially oxidized to the corresponding ketones in the presence of anionic peroxomolybdenum complexes^[19]. However, conversion of the OH function of **1** into a carbonyl group can be achieved quantitatively by Swern oxidation^[20]. Oxidation of enantiomerically pure (1*S*,2*S*)-**1** yields a racemic mixture of **3** under these conditions. We are interested in such compounds as building blocks for chiral multidentate ligands and are therefore currently working on the resolution of *rac-3*. The corresponding peroxomolybdenum complex **4** is available in a similar way to **2** by simply stirring a peroxidic solution of molybdic acid with a solution of **3** in dichloromethane (Scheme 3).

NMR spectroscopy shows that the peroxo complex **4** exists in chloroform solution as a 4.5:1 mixture of the two isomers **A** and **B**. This gives an indication of the slightly stronger electron-withdrawing properties of the β -oxo group compared to the β -hydroxy group of **1**, favoring the population of isomer **A**. The corresponding peroxo complex

Scheme 3. i. $(\text{CH}_3)_2\text{SO}$, $(\text{COCl})_2$, NEt_3 , -72°C , CH_2Cl_2 ;
ii. $\text{MoO}_3 \cdot (\text{H}_2\text{O})_x$, H_2O_2 , room temp., 4 h



4 catalyzes the epoxidation of olefins in the presence of *tert*-butyl hydroperoxide, showing an activity comparable to that of other peroxomolybdenum complexes^[6].

Conclusion

Proton-transfer reactions play an important role in many organic transformations catalyzed by high-valent transition-metal centers. From a mechanistic point of view, hydrogen-bond formation can be considered as the primary step in such reactions. With the synthesis of *trans*-2-[3-(2-pyridyl)-1-pyrazolyl]cyclohexanol (**1**), we succeeded not only in establishing a new chiral polydentate ligand system with potential applications in enantioselective catalysis, but were also able to obtain thermodynamic information on the strength of an $\text{Mo}^{\text{VI}}(\eta^2\text{-O}_2) \cdots \text{HO}-\text{C}$ interaction. Such an interaction in solution has never been described in detail before. Owing to the low Lewis basicity of the peroxo ligand coordinated to a high-valent transition-metal center this interaction is weak and can therefore be broken by Lewis-basic solvents. In the solid state, this hydrogen bond is no longer intramolecular but intermolecular. The formation of the intramolecular hydrogen bond in solution allowed a new assignment of the NMR data of pyrazolylpyridine peroxomolybdenum complexes. A simple and high-yield transformation of the secondary alcohol **1** into the ketone **3** led to a new chiral building block for multidentate ligand systems. The potential of such a system as a metal-complexing agent was proved by the formation of the corresponding peroxo complex **4**.

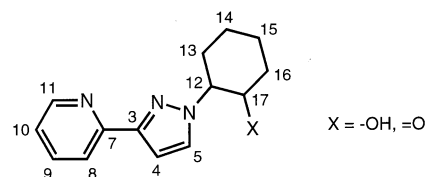
The authors wish to thank Prof. W. A. Herrmann, the Deutsche Forschungsgemeinschaft and the Fonds der Chemischen Industrie for

support of this work, and Henricke Heise for performing the CPMAS experiments.

Experimental Section

2-[3(5)-Pyrazolyl]pyridine was synthesized according to a published procedure^[3]. Immobilized lipase B from *candida antarctica* was a generous gift from Novo Nordisk. All other starting materials were purchased from Aldrich. Isopropenyl acetate was distilled from K_2CO_3 before use. The NMR (Bruker DPX 400), infrared (Perkin-Elmer 1600 Series FTIR) and mass spectra (GC MS: Hewlett-Packard gas chromatograph HP 5890 and mass selective detector HP 5970), and all elemental analyses were carried out at the Anorganisch-chemisches Institut der TU München. The numbering of the NMR spectra is carried out according to Scheme 4.

Scheme 4. Labeling scheme for the assignment of NMR data



rac-[3-(2-Pyridyl)-1-pyrazolyl]cyclohexanol (*rac*-**1**): A mixture of 2-[3(5)-pyrazolyl]pyridine (2.0 g, 13.9 mmol) and epoxycyclohexane (2.0 g, 2.1 ml, 20.8 mmol) was heated for 4 h at 170°C in a pressure tube (Aldrich Z18,108-0). The dark-colored product was dissolved in dichloromethane and treated with 5.0 g of silica gel. The solvent was removed in vacuo and the powdery product transferred to a Soxhlet extractor. Extraction with diethyl ether and removal of the solvent yielded **1** (3.1 g, 92%) as a pale yellow oil. – IR (KBr, cm^{-1}): $\tilde{\nu} = 3382$ s, br. (OH), 2935 vs, 2857 s, 1595 vs, 1567 m, 1490 s, 1459 s, 1432 m, 1410 m, 1365 m, 1278 m, 1264 w, 1229 s, 1149 w, 1074 s, 1000 w, 954 m, 870 w, 797 m, 765 vs, 708 w, 644 w, 621 w. – ^1H NMR (400 MHz, 25°C , CDCl_3): $\delta = 8.55$ (d, $^3J_{10,11} = 5.0$ Hz, 11-H), 7.88 (d, $^3J_{8,9} = 8.0$ Hz, 8-H), 7.65 (dt, $^3J_{9,10} = 7.5$ Hz, $^4J_{9,11} = 2.0$ Hz, 9-H), 7.47 (d, $^3J_{4,5} = 2.5$ Hz, 5-H), 7.13 (dd, 10-H), 6.85 (d, 4-H), 3.91 (m, 12-H, 13-H), 2.14 (m, $-\text{CH}_2-$, 2 H), 1.87–1.18 (m, $-\text{CH}_2-$, 6 H), not observed (OH). – $^{13}\text{C}\{^1\text{H}\}$ NMR (100.6 MHz, 25°C , CDCl_3): $\delta = 152.1$ (C-7), 151.4 (C-3), 149.2 (C-11), 136.5 (C-9), 129.7 (C-5), 122.3 (C-10), 120.0 (C-8), 104.0 (C-4), 72.9 (C-17), 67.2 (C-12), 33.3 (C-16), 31.0 (C-13), 24.8 (C-14), 23.9 (C-15). – MS (EI); m/z (%): 243 (25) [M^+], 226 (2) [$\text{M}^+ - \text{OH}$], 215 (25) [$\text{M}^+ - \text{C}_2\text{H}_4$], 200 (6) [$\text{M}^+ - \text{C}_3\text{H}_7$], 187 (13) [$\text{M}^+ - \text{C}_4\text{H}_8$], 172 (100) [$\text{M}^+ - \text{C}_4\text{H}_7\text{O}$], 158 (51) [$\text{M}^+ - \text{C}_5\text{H}_9\text{O}$], 146 (46) [$\text{C}_5\text{H}_4\text{N}-\text{C}_3\text{H}_3\text{N}_2^+$], 145 (25) [$\text{C}_5\text{H}_4\text{N}-\text{C}_3\text{H}_2\text{N}_2^+$], 117 (14) [$\text{C}_5\text{H}_4\text{N}-\text{C}_3\text{H}_2^+$], 78 (22) [$\text{C}_5\text{H}_4\text{N}^+$].

(1*S*,2*S*)-[3-(2-Pyridyl)-1-pyrazolyl]cyclohexanol Hydrate [(1*S*,2*S*)-**1**· H_2O]: *rac*-**1** (0.50 g, 2.06 mmol) was dissolved in isopropenyl acetate (1.36 ml, 1.24 g, 12.36 mmol). Molecular sieves (4 Å, 0.5 g) and immobilized lipase B from *candida antarctica* (16 mg) were added and the mixture stirred for 4 h at 37°C . The reaction was quenched by the addition of dichloromethane (15 ml) and the enzyme filtered off. All volatile material was removed in vacuo and the ester separated from the alcohol by MPLC (SiO_2 :YMC SL06S21, 30 μm ; ethyl acetate/hexane 4:1). Yield: 0.22 g (44%, > 95% ee by NMR) of (1*S*,2*S*)-**1**. Recrystallization from diethyl ether gave colorless plates of the monohydrate. – $\text{C}_{14}\text{H}_{17}\text{N}_3\text{O} \cdot \text{H}_2\text{O}$ (261.33): calcd. C 64.35, H 7.33, N 16.08; found C 63.29, H 7.20, N 15.55.

rac- and (1*S*,2*S*)-Oxodiperoxo{[3-(2-pyridyl)-1-pyrazolyl]cyclohexanol}molybdenum(VI) [*rac*- and (1*S*,2*S*)-**2**]: A solution of

molybdic acid ($\text{MoO}_3 \cdot \text{H}_2\text{O}$, 0.41 g, 2.56 mmol) in 30% H_2O_2 (5 ml) was treated with a solution of *rac*-**1** or (1*S*,2*S*)-**1** (0.31 g, 1.28 mmol) in dichloromethane (10 ml) and several drops of glacial acetic acid. After 4 h of stirring at room temperature, the phases were separated, the aqueous phase was extracted twice with dichloromethane (10 ml) and the combined organic phases were washed twice with water (15 ml). After removal of the solvent in vacuo, the peroxo complexes were obtained as yellow, microcrystalline solids in almost quantitative yields, and were rinsed with diethyl ether. Recrystallization of *rac*-**2** from acetonitrile gave a crystalline material (0.37 g, 69%). – IR (KBr, cm^{-1}): $\tilde{\nu}$ = 3489 vs br. (OH), 3138 w, 3084 w, 2926 m, 2854 w, 1612 m, 1559 w, 1540 w, 1506 w, 1457 w, 1437 m, 1376 w, 1224 w, 1083 w, 1062 w, 956 s ($\text{Mo}=\text{O}$), 871 m, 859 s ($2 \times \text{O}-\text{O}$), 770 m, 662 w, 587 m, 540 w. – ^1H NMR (400 MHz, 25°C, CDCl_3): δ = 9.30 (d, $^3J_{10,11}$ = 5.5 Hz, 11-H), 8.23 (dt, $^3J_{8,9}$ = $^3J_{9,10}$ = 8.0 Hz, $^4J_{9,11}$ = 1.5 Hz, 9-H), 7.92 (d, 8-H), 7.65 (t, 10-H), 7.42 (d, $^3J_{4,5}$ = 2.5 Hz, 5-H), 6.77 (d, 4-H), 4.33 (dt, $^3J_{12,13\text{ax}}$ = $^3J_{12,17}$ = 10.5 Hz, $^4J_{12,13\text{eq}}$ = 2.5 Hz, 12-H), 3.37 (dt, $^3J_{16,17\text{ax}}$ = 10.5 Hz, $^4J_{16,17\text{eq}}$ = 2.5 Hz, 17-H), 2.78–1.20 (m, $-\text{CH}_2-$, 8 H). – ^1H NMR (400 MHz, 25°C, $[\text{D}_6]\text{acetone}$): isomer A: δ = 9.27 (d, $^3J_{10,11}$ = 5.0 Hz, 11-H), 8.53 (dt, $^3J_{8,9}$ = $^3J_{9,10}$ = 8.0 Hz, $^4J_{9,11}$ = 1.5 Hz, 9-H), 8.38 (d, 8-H), 7.92 (t, 10-H, 5-H), 7.13 (d, $^3J_{4,5}$ = 2.5 Hz, 4-H), 4.26 (dt, $^3J_{12,13\text{ax}}$ = $^3J_{12,17}$ = 12.0 Hz, $^4J_{12,13\text{eq}}$ = 4.0 Hz, 12-H), 3.70 (m, 17-H), 2.80–1.20 (m, $-\text{CH}_2-$, 8 H); isomer B: δ = 8.66 (d, $^3J_{10,11}$ = 5.0 Hz, 11-H), 8.17 (d, $^3J_{8,9}$ = 7.5 Hz, 8-H), 8.05 (m, 9-H, 5-H), 7.48 (d, $^3J_{4,5}$ = 2.5 Hz, 4-H), 7.42 (ddd, $^3J_{9,10}$ = 7.0 Hz, $^4J_{8,10}$ = 2.0 Hz, 10-H), 5.13 (dt, $^3J_{12,13\text{ax}}$ = $^3J_{12,17}$ = 12.5 Hz, $^4J_{12,13\text{eq}}$ = 4.0 Hz, 12-H), 3.35 (m, 17-H), 2.80–1.20 (m, $-\text{CH}_2-$, 8 H). – $^{13}\text{C}\{^1\text{H}\}$ NMR (100.6 MHz, 25°C, CDCl_3): δ = 154.7 (C-11), 149.4 (C-7), 143.8 (C-3), 142.8 (C-9), 129.2 (C-5), 125.0 (C-10), 122.5 (C-8), 105.0 (C-4), 75.1 (C-17), 67.7 (C-12), 35.8 (C-16), 31.9 (C-13), 24.9 (C-14), 24.8 (C-15). – ^{13}C CPMAS (75.468 MHz, 25°C): δ = 155.9 (C-11), 150.2 (C-7), 145.7 (C-3, C-9), 130.7 (C-5), 124.0 (C-10), 122.6 (C-8), 104.5 (C-4), 67.8 (C-17, C-12), 35.7 (C-16, C-13), 25.2 (C-14, C-15). – $\text{C}_{14}\text{H}_{17}\text{N}_3\text{O}_6\text{Mo}$ (419.25): calcd. C 40.11, H 4.09, N 10.02; found C 40.16, H 4.13, N 10.09.

rac-[3-(2-Pyridyl)-1-pyrazolyl]cyclohexanone (*rac*-**3**): Dimethyl sulfoxide (0.75 ml, 0.88 g, 11.3 mmol) was added to a solution of **1** (1.15 g, 4.73 mmol) in dichloromethane (30 ml) at -72°C . After 30 min, oxalyl chloride (1.33 ml, 1.93 g, 15.2 mmol) was added dropwise and, after a further 60 min, triethylamine (2.92 ml, 2.22 g, 21.9 mmol) was added. The reaction mixture was stirred for a further 60 min at -60°C and the reaction was quenched with water (1 ml). The mixture was extracted twice with dichloromethane (30 ml), the combined organic phases washed with brine, dried with MgSO_4 and the solvent was removed in vacuo. Recrystallization from diethyl ether gave **3** (1.11 g, 97%) as colorless needles. – IR (KBr, cm^{-1}): $\tilde{\nu}$ = 3131 w, 2940 s, 2864 m, 1725 vs (CO), 1593 s, 1567 w, 1490 m, 1458 m, 1430 w, 1366 m, 1278 w, 1222 m, 1128 w, 1051 w, 992 w, 956 w, 767 s, 710 w, 622 w. – ^1H NMR (400 MHz, 25°C, CDCl_3): δ = 8.59 (d, $^3J_{10,11}$ = 54.5 Hz, 11-H), 7.85 (d, $^3J_{8,9}$ = 8.0 Hz, 8-H), 7.66 (dt, $^3J_{9,10}$ = 7.5 Hz, $^4J_{9,11}$ = 2.0 Hz, 9-H), 7.47 (d, $^3J_{4,5}$ = 2.0 Hz, 5-H), 7.15 (dd, 10-H), 6.92 (d, 4-H), 5.13 (dd, $^3J_{12,13\text{ax}}$ = 13.0 Hz, $^3J_{12,13\text{eq}}$ = 4.5 Hz, 12-H), 2.63–1.70 (m, $-\text{CH}_2-$, 8 H). – $^{13}\text{C}\{^1\text{H}\}$ NMR (100.6 MHz, 25°C, CDCl_3): δ = 204.7 (C-17), 152.1 (C-7), 151.1 (C-3), 149.4 (C-11), 136.4 (C-9), 130.3 (C-5), 122.3 (C-10), 120.1 (C-8), 104.7 (C-4), 69.6 (C-12), 41.3 (C-16), 34.6 (C-13), 27.2 (C-14), 24.7 (C-15). – MS (EI); m/z (%): 241 (37) [M^+], 213 (8) [$\text{M}^+ - \text{CO}$], 198 (5) [$\text{M}^+ - \text{C}_3\text{H}_7$], 185 (6) [$\text{M}^+ - \text{C}_4\text{H}_8$], 184 (9) [$\text{M}^+ - \text{C}_3\text{H}_5\text{O}$], 172 (63) [$\text{M}^+ - \text{C}_5\text{H}_9$], 170 (4) [$\text{M}^+ - \text{C}_4\text{H}_7\text{O}$], 158 (20) [$\text{C}_5\text{H}_4\text{N}-\text{C}_3\text{H}_2\text{N}_2-\text{CH}_3^+$], 145 (100) [$\text{C}_5\text{H}_4\text{N}-\text{C}_3\text{H}_2\text{N}_2^+$], 117 (13) [$\text{C}_5\text{H}_4\text{N}-\text{C}_3\text{H}_2^+$], 78

(25) [$\text{C}_5\text{H}_4\text{N}^+$]. – $\text{C}_{14}\text{H}_{15}\text{N}_3\text{O} \cdot 0.25\text{H}_2\text{O}$ (245.79): calcd. C 68.41, H 6.36, N 17.09; found C 68.65, H 6.02, N 16.93.

rac-Oxodiperoxo{[3-(2-pyridyl)-1-pyrazolyl]cyclohexanone}molybdenum(VI) (*rac*-**4**): A solution of molybdic acid ($\text{MoO}_3 \cdot \text{H}_2\text{O}$, 0.34 g, 1.90 mmol) in 30% H_2O_2 (5 ml) was treated with a solution of *rac*-**3** (0.25 g, 0.95 mmol) in dichloromethane (10 ml) and several drops of glacial acetic acid. After 4 h of stirring at room temperature, the phases were separated, the aqueous phase was extracted twice with dichloromethane (10 ml) and the combined organic phases were washed twice with water (15 ml). After removal of the solvent in vacuo followed by washing with diethyl ether, the product was obtained as a yellow, microcrystalline solid in almost quantitative yield. – IR (KBr, cm^{-1}): $\tilde{\nu}$ = 3124 m, 2934 m, 2869 w, 1732 s (CO), 1616 s, 1567 w, 1532 w, 1504 w, 1442 m, 1395 m, 1383 w, 1297 w, 1241 m, 1165 w, 1127 w, 1103 m, 1081 w, 1029 w, 977 w, 955 vs ($\text{Mo}=\text{O}$), 876 m, 865 vs ($2 \times \text{O}-\text{O}$), 777 s, 665 m, 585 m, 540 w. – ^1H NMR (400 MHz, 25°C, $[\text{D}_6]\text{acetone}$): isomer A: δ = 9.23 (d, $^3J_{10,11}$ = 5.5 Hz, 11-H), 8.20 (dt, $^3J_{8,9}$ = $^3J_{9,10}$ = 8.0 Hz, $^4J_{9,11}$ = 1.2 Hz, 9-H), 7.91 (d, 8-H), 7.62 (dd, 10-H), 7.40 (d, $^3J_{4,5}$ = 2.5 Hz, 5-H), 6.72 (d, 4-H), 5.41 (dd, $^3J_{12,13\text{ax}}$ = 13.6 Hz, $^3J_{12,13\text{eq}}$ = 5.5 Hz, 12-H), 2.80–1.55 (m, $-\text{CH}_2-$, 8 H); isomer B: δ = 8.60 (br, 11-H), 8.05 (d, $^3J_{4,5}$ = 3.0 Hz, 5-H), 7.83 (d, $^3J_{8,9}$ = 8.0 Hz, 8-H), 7.77 (dt, $^3J_{9,10}$ = 7.5 Hz, $^4J_{9,11}$ = 1.5 Hz, 9-H), 7.19 (dd, 10-H), 7.04 (d, 4-H), 6.17 (dd, $^3J_{12,13\text{ax}}$ = 13.6 Hz, $^3J_{12,13\text{eq}}$ = 5.5 Hz, 12-H), 2.80–1.55 (m, $-\text{CH}_2-$, 8 H); isomer ratio A:B = 4.5:1. – $^{13}\text{C}\{^1\text{H}\}$ NMR (100.6 MHz, 25°C, $[\text{D}_6]\text{acetone}$): isomer A: δ = 203.2 (C=O), 154.5 (C-11), 150.9 (C-7), 144.5 (C-3), 142.9 (C-9), 132.1 (C-5), 125.1 (C-10), 122.8 (C-8), 104.3 (C-4), 68.9 (C-12), 41.2 (C-16), 34.9 (C-13), 27.6 (C-14), 24.6 (C-15); isomer B: δ = 202.7 (C=O), 147.2 (C-11), 139.2 (C-9), 136.9 (C-5), 125.1 (C-10), 120.7 (C-8), 105.1 (C-4), not detected (C-3, C-7), 68.5 (C-12), 40.8 (C-16), 34.6 (C-13), 27.1 (C-14), 24.4 (C-15). – $\text{C}_{14}\text{H}_{15}\text{N}_3\text{O}_6\text{Mo}$ (417.23): calcd. C 40.30, H 3.62, N 10.07; found C 40.35, H 3.83, N 9.88.

*Crystallographic Structure Determination and Structure Refinement of (1*S*,2*S*)-1 · H₂O and rac-2*: The crystals were fixed inside a Lindemann glass capillary. The intensity data were obtained at 293 K with graphite-monochromated Mo-K_α radiation using a STOE IPDS^[21] in the case of *rac*-**2** and at 193 K with graphite-monochromated Cu-K_α radiation using an Enraf Nonius CAD4^[22] diffractometer in the case of (1*S*,2*S*)-**1**. A combined absorption and decay correction, using the program DECAY^[21] (smooth factor 8) was applied on the data set of *rac*-**2**. During the data collection for (1*S*,2*S*)-**1**, three standard reflections lost 12% of intensity, which was corrected with the program MolEN^[22]. Preliminary positions of heavy atoms were found by direct methods (SIR92^[23]), while positions of the other non-hydrogen atoms were determined from successive Fourier difference maps coupled with an initial isotropic least-squares refinement (SHELXL93^[24]). The hydrogen atoms of (1*S*,2*S*)-**1** were all located in the difference Fourier maps and refined with isotropic temperature parameters. In the case of *rac*-**2** all hydrogen atoms were placed in calculated positions, included in the structure-factor calculation, but were not refined. Additional crystal data, data collection and refinement parameters are presented in Table 1.

Crystallographic data (excluding structure factors) for the structures reported in this paper have been deposited with the Cambridge Crystallographic Data Centre (CCDC-100572). Copies of the data may be obtained free of charge on application to CCDC, 12 Union Road, Cambridge CB2 1EZ, UK [fax: int. code + (1223)336-033; e-mail: deposit@ccdc.cam.ac.uk].

X-ray Powder Diffraction: The X-ray diffraction pattern was recorded with a Huber Guinier diffractometer 642 with Ge mono-

Table 1. Crystal data and collection parameters for compounds (1*S*,2*S*)-**1** and *rac*-**2**

	(1 <i>S</i> ,2 <i>S</i>)- 1	<i>rac</i> - 2
empirical formula	C ₁₄ H ₁₉ N ₃ O ₂	C ₁₄ H ₁₇ MoN ₃ O ₆
formula weight [a.m.u]	261.32	419.25
color, habit	colorless plates	yellow needles
crystal system	monoclinic	orthorhombic
space group	<i>P</i> 2 ₁ (no. 4)	<i>P</i> ca2 ₁ (no. 29)
<i>a</i> [Å]	9.4298(11)	13.4166(11)
<i>b</i> [Å]	7.2854(4)	13.8384(9)
<i>c</i> [Å]	10.5036(12)	8.3365(5)
β [°]	106.692(6)	90.00
<i>V</i> [Å ³]	691.19(12)	1547.8(2)
<i>Z</i>	2	4
calcd. density [g cm ⁻³]	1.256	1.799
μ [mm ⁻¹]	0.694	0.885
<i>F</i> (000)	280	848
<i>T</i> [°C]	193(2)	293(2)
radiation type	Cu- <i>K</i> α	Mo- <i>K</i> α
diffractometer	CAD4	STOE IPDS
data collection range	2 < Θ < 68	1.6 < Θ < 26.0
number of reflections collected	4886	12686
number of unique reflections	2491	2472
number of refl. used for refinem.	2491	2472
observation criteria	<i>I</i> > $\sigma(I)$	<i>I</i> > $\sigma(I)$
refined parameters	224	217
reflections/parameter	10.22	10.01
Flack parameters	−0.06(21)	−0.01(5)
final <i>R</i> 1	0.0401	0.0309
final ωR 2	0.0872	0.0714
GOF	1.065	1.176
largest remaining feature in electron density map	0.163/−0.272	0.538/−0.503

chromator ($\lambda = 154.056$ pm) at 293 K with a 5-s scan time and 0.01° step width (step-scanning method). Selected data: space group: orthorhombic, *P*ca2₁ (no. 29); *a* = 13.4682, *b* = 13.8860, *c* = 8.1370 Å; *V* = 1521.78 Å³; most intense reflections (*hkl*/ Θ value/rel. intensity): 010/3.18°/9.1%, 110/4.57°/5.4%, 020/6.35°/25.2%, 200/6.58°/37.4%, 111/6.97°/100%, 121/8.89°/76.1%, 221/10.55°/12.6%, 230/11.67°/23.8%.

[1] W. R. Thiel, J. Eppinger, *Chem. Eur. J.* **1997**, 3, 696–705.

[2] [2a] *Organic Synthesis by Oxidation with Metal Compounds* (Eds.: W. J. Mijss, C. H. R. T. de Jonge), Plenum Press, New York, **1986**. — [2b] R. A. Sheldon in *The Chemistry of Peroxides* (Ed.: S. Patai), Wiley, New York, **1983**.

[3] H. Brunner, T. Scheck, *Chem. Ber.* **1992**, 125, 701–709.

[4] W. R. Thiel, T. Priermeier, *Angew. Chem.* **1995**, 107, 1870–1871; *Angew. Chem. Int. Ed. Engl.* **1995**, 34, 1737–1738.

[5] W. R. Thiel, *Chem. Ber.* **1996**, 129, 575–580.

[6] W. R. Thiel, M. Angstl, T. Priermeier, *Chem. Ber.* **1994**, 127, 2373–2379.

[7] [7a] H. Kotsuki, H. Hayakawa, M. Wakao, T. Shimanouchi, M. Ochi, *Tetrahedron Asymm.* **1995**, 6, 2665–2668. — [7b] H. Kotsuki, K. Hayashida, T. Shimanouchi, H. Nishizawa, *J. Org. Chem.* **1996**, 61, 984–990. — [7c] P. Barbaro, C. Bianchini, V. Sernau, *Tetrahedron Asymm.* **1996**, 7, 843–850.

[8] [8a] P. Barbaro, C. Bianchini, V. Sernau, *Tetrahedron Asymm.* **1996**, 7, 843–850. — [8b] C. L. Thurner, M. Barz, M. Spiegler, W. R. Thiel, *J. Organomet. Chem.* **1997**, 541, 39–49. — [8c] C. L. Thurner, M. Barz, M. Spiegler, W. R. Thiel, *Acta Crystallogr. C*, in press.

[9] M. Barz, M. U. Rauch, W. R. Thiel, *J. Chem. Soc., Dalton Trans.* **1997**, 2155–2161.

[10] M. Barz, E. Herdtweck, W. R. Thiel, *Tetrahedron Asymm.* **1996**, 7, 1717–1722.

[11] [11a] T. V. Hansen, V. Waagen, V. Partali, H. W. Anthonson, T. Anthonson, *Tetrahedron Asymm.* **1995**, 6, 499–504. — [11b] H. Frykman, N. Öhrner, T. Norin, K. Hult, *Tetrahedron Lett.* **1993**, 34, 1367–1370. — [11c] G. Nicolosi, A. Patti, M. Piattelli, C. Sanfilippo, *Tetrahedron Asymm.* **1995**, 6, 519–524. — [11d] H. Sundram, A. Golebbiowski, C. R. Johnson, *Tetrahedron Lett.* **1994**, 35, 6975–6976.

[12] A. L. Spek, *Acta Crystallogr. C* **1990**, A46, C34–C34.

[13] H. D. Flack, *Acta Crystallogr. C* **1983**, A39, 876–881.

[14] M. Mattner, PhD Thesis, TU München, **1995**.

[15] S. N. Vinogradov, R. H. Linnell, *Hydrogen Bonding*, Van Nostrand Reinhold Company, New York, **1971**.

[16] W. Winter, C. Mark, V. Schurig, *Inorg. Chem.* **1980**, 19, 2045–2049.

[17] [17a] E. O. Schlemper, G. N. Schrauzer, L. A. Hughes, *Polyhedron* **1984**, 3, 377–380. — [17b] W. A. Herrmann, W. R. Thiel, J. G. Kuchler, J. Behm, E. Herdtweck, *Chem. Ber.* **1990**, 123, 1963–1970.

[18] Data for the plate-like crystals: crystal system, monoclinic; space group, *P*2₁/*c* (int. table no. 14); *a* = 13.4460(8); *b* = 8.4082(3); *c* = 15.1809(8) Å; β = 115.328(5)°; *V* = 1551.32(15) Å³; *Z* = 4; *D*_{calcd.} = 1.778 g cm⁻³; *F*(000) = 832; μ = 8.8 cm⁻¹; *T* = 193 K; Mo-*K* α radiation; STOE IPDS; oscillation mode; *h*, *k*, *l*: −16/16, −10/10, −18/18; total no. of refl.: 17095; no. of unique refl.: 2934; no. of observed refl.: 2357; no. of parameters: 221, *R* = 0.0993, ωR 2 = 0.2780; GOF = 1.23; res. electr. densities: −1.38/+2.57; additional material is available from the authors.

[19] *Catalytic Oxidations with Hydrogen Peroxide as Oxidant* (Ed.: G. Strukul), Kluwer Academic Publishers, Rotterdam, **1992**.

[20] J. A. Mancuso, S.-L. Huang, D. Swern, *J. Org. Chem.* **1978**, 43, 2480–2482.

[21] STOE & CIE GmbH, *IPDS Operating System, Version 2.6*, Darmstadt, **1995**.

[22] Enraf-Nonius, *CAD4 Software, Version 5*, Delft, **1989**.

[23] A. Altomare, G. Cascarano, C. Giacovazzo, A. Guagliardi, *J. Appl. Crystallogr. C* **1993**, 26, 343–350.

[24] G. Sheldrick, *SHELXL 93*, Universität Göttingen, **1993**.

[97167]